Macromolecules
COMMUNICATION TO THE EDITOR

Macromolecules **2009**, *42*, 5437–5441 **5437**
DOI: 10.1021/ma900669r

Direct Formation and Characterization of a Unique Precursor Morphology in the Melt-Spinning of Polyesters

Peng Chen,[†,‡] Mehdi Afshari,[‡] John A. Cuculo,*[,‡] and Richard Kotek*[,‡]

[†]*Ningbo Institute of Materials Technology and Engineering, Chinese Academy of Sciences, Ningbo, Zhejang 315201, People's Republic of China, and* [‡]*College of Textiles, Textile Engineering, Chemistry, and Science Department, North Carolina State University, Raleigh, North Carolina 27695*

Received March 30, 2009
Revised Manuscript Received July 3, 2009

Introduction. Recently a precursor for crystallization has been intensively reported for polyesters, such as poly(ethylene terephthalate) (PET),[1−13] poly(ethylene naphthalate) (PEN),[1,2,14−16] and their copolymers.[1,2,17,18] Under various conditions, the precursor was found to take nematic,[8,11] smectic,[1−3,8−14,17,18] or unidentified forms,[4−7,15,16] sometimes accompanied by microvoids[14,19] and banded structure.[18,20] Since the formation of the precursor was transient and extremely sensitive to processing conditions, it was not surprising that the observed forms of the precursor were so diverse. However, all the forms had a feature in common that they consisted of highly oriented, yet noncrystallized molecular chains or chain segments. We realized that this feature of the precursor would be very useful in solving the major problem of the traditional melt-spinning process, i.e., the occurrence of crystallization during spinning and drawing which reduces the chain mobility and interrupts the development of molecular orientation, resulting in limited fiber properties.

In most studies,[1−20] the occurrence of the precursor was observed by drawing the polyester samples at a temperature close to the glass transition temperature (T_g) and at a high strain and stain rate. Apparently, this is also presumed to happen during the practical melt-spinning and drawing process when certain conditions are satisfied. Nevertheless, the transformation was usually difficult to detect because of the rapid transformation occurring from the precursor to normal crystals. To observe or even produce fibers consisting mainly of the precursor structure, it is necessary to extend the lifetime of the precursor while retarding the crystallization in the threadline. In this work, a liquid isothermal bath (LIB), which has been described elsewhere,[21] was used to fulfill this requirement. As a result, PET and PEN fibers showing unique precursor morphology were directly produced in the melt-spinning process. Then superior fiber properties were achieved by drawing the fibers spun with LIB to a low draw ratio. Therefore, the work serves to confirm the ability of PET and PEN to form precursors for crystallization under specific conditions, as theoretically predicted[22,23] and experimentally observed before only in specialized laboratory experiments.[1−20] This work also provides the initial example of producing fibers with improved properties by the well-controlled generation of the precursor morphology using the practicable melt-spinning process.

*Corresponding authors. E-mail: John_Cuculo@ncsu.edu (J.A.C.); rkotek@ncsu.edu (R.K.).

Experimental Section. *Sample Preparation*. PET and PEN chips were used in this work, having intrinsic viscosity (IV) of 0.97 and 1.0 dL/g, respectively, as measured in 60/40 w/w phenol/tetrachloroethane solution. Both polymers were vacuum-dried at 140 °C for 16 h before use. A Fourne single-screw extruder, equipped with a single-hole, hyperbolic spinneret with 0.6 mm exit diameter, was used for melt-extrusion and spinning. The spinneret temperature was set at 290 °C for PET and 310 °C for PEN. After emergence from the spinneret, the filament was directed into a liquid isothermal bath (LIB), which has been described elsewhere,[21] and wound at 1000−4000 m/min. The fibers spun with LIB were then drawn by using a modified Instron tensile testing machine equipped with a 60 cm long heating tube. The draw speed was 5 cm/min, and the draw temperature was 120 °C for PET and 160 °C for PEN.

Measurements. Wide-angle X-ray diffraction (WAXD) measurements were performed on a Siemens type F diffractometer system with Cu Kα radiation generated at 30 kV and 20 mA. The diffracting intensities were recorded every 0.1° from 2θ scans in the range 5°−40°. The crystalline and amorphous orientation factors (f_c, f_a) was calculated using traditional methods as described previously.[21] The density of fiber samples was measured by using a density gradient column consisting of aqueous sodium bromide maintained at 23 ± 0.1 °C. Tensile properties of fibers were measured on an MTS testing machine following ASTM D3822. A gage length of 25.4 mm and a constant cross-head speed of 15 mm/min were adopted. Fiber samples were broken in liquid nitrogen, and the cross section as well as surface of the samples was observed on a Hitachi S-3200 scanning electron microscope (SEM). To study the inner morphology, fiber samples were cut in both radial and longitudinal directions via a focus ion beam (FIB) technology. High-resolution images were taken by using a Hitachi Su-70 field emission SEM.

Results and Discussion. During the melt-spinning of PET and PEN fibers with LIB, it was noted that the fibers turned white under certain conditions. A number of trials showed that the fiber whitening was dominated by three factors, namely, time, tension, and temperature. To be specific, it was necessary to maintain a sufficiently high tension in the threadline at a temperature close to T_g for a suitable time to produce white fibers. For example, by placing the LIB device 110 cm below the spinneret, with liquid depth fixed at 25 cm, and using a take-up speed of 4000 m/min, the PET white fibers were produced at a liquid temperature of 80 °C while the PEN white fibers were produced at a liquid temperature of 135 °C. The white fibers showed very unique properties, and in this Communication we want to take the PEN fibers as a typical example. (For details on fiber properties and morphology of PET, see Supporting Information.)

One of the most attractive properties of the white fibers spun with LIB is their high tenacity but low modulus and high elongation, as shown in Table 1. In fact, the tenacity of the PEN fibers spun at 4000 m/min with LIB is almost 40% higher than that of the normal fibers spun without LIB. At the same time, the modulus is low and the elongation remains high for the white fibers, which implies that the fibers may be drawn further.

Table 1 also shows the properties of the PEN drawn fibers spun with and without LIB. As expected, both fibers can be

Published on Web 07/10/2009

Table 1. Properties of PEN Fibers Spun at 4000 m/min

fiber sample		tenacity (g/d)	modulus (g/d)	elongation (%)	X_c[a] (%)	X_c[b] (%)	f_c	f_a
undrawn	no LIB	5.35	126.2	11.7	27.0	30.5	0.92	0.72
	LIB	7.27	114.5	12.8	0	7.4	0.93	0.82
drawn (DR = 1.40)	no LIB	7.31	173.0	8.7	35.2	39.4	0.95	0.78
	LIB	10.75	216.7	7.6	49.6	51.3	0.97	0.90

[a] The crystallinity is calculated by using density data. [b] The crystallinity is calculated by using WAXD data.

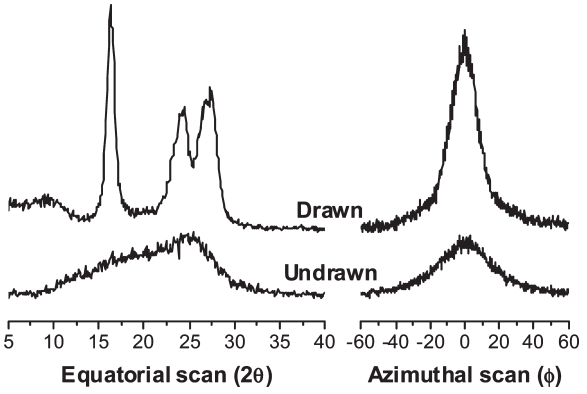

Figure 1. Equatorial and azimuthal X-ray diffraction profiles of undrawn (lower) and drawn (upper) PEN fibers spun with LIB.

drawn to a draw ratio (DR) of 1.40, resulting in increased tenacity and modulus as well as decreased elongation. However, the LIB fibers gain much more improvement in fiber properties. For example, the tenacity and the modulus are increased by ca. 50% and 90%, and the elongation is decreased by 40%, respectively, for the LIB fibers. Of most interest is the high tenacity (10.75 g/d) and modulus (216.7 g/d) of the LIB drawn fibers at a low draw ratio (1.40). Normally much higher draw ratios (5−7) are necessary in the traditional melt spin-draw process to reach the same high level fiber tenacity and modulus.[24]

In addition to the superior mechanical properties, the LIB fibers also show very unique morphology. Note in Table 1 that the crystallinity calculated from density is zero for the undrawn fibers spun with LIB. In other words, the LIB undrawn fibers show low density and seem to be totally amorphous. This is quite surprising because the LIB fibers show high tenacity and the high-speed spun fibers, as usually expected, should be highly crystallized, especially with the threadline tension enhanced by the LIB device.

The direct way to determine whether the LIB fibers are amorphous or crystalline is through wide-angle X-ray diffraction (WAXD). WAXD profiles of the undrawn and drawn PEN fibers spun with LIB are shown in Figure 1. Interestingly, the equatorial X-ray diffraction profile of the LIB undrawn fibers is diffuse, indicating very low crystallinity. In contrast, the drawn fibers show distinct crystal peaks and adopt the α modification. The azimuthal scan is also shown in Figure 1 for a characterization of chain orientation. It can be seen that the drawn fibers show sharp and strong peak in azimuthal scan, suggesting a well-developed chain orientation. At the same time, the undrawn fibers spun with LIB show a mild peak in azimuthal scan, implying a certain extent of chain orientation. The calculated orientation factors (Table 1) confirm that the undrawn LIB fiber show much higher amorphous orientation than the undrawn fibers spun without LIB. Therefore, the WAXD data clearly indicate that the LIB undrawn fibers of PEN show an amorphous but oriented feature, which turns into a highly crystallized and oriented feature for the drawn fibers.

Accompanied with the crystallization during drawing the LIB fibers, another interesting phenomenon drew our attention and led to in-depth morphological studies. That is, the white color of the LIB undrawn fibers gradually faded during hot drawing. To investigate the color change process, we drew a single fiber by using the heating tube and selected three zones along the fiber for observation. The undrawn zone was outside the tube, where the fiber was unheated and retained the white color; the drawn zone was in the tube, where the fiber was fully heated and drawn and transparent in appearance; the transit zone between undrawn and drawn was on the lower edge of the tube end, where the fiber was translucent.

Figure 2 shows SEM images of the three zones of the PEN fiber. As Figure 2a shows, the undrawn white fiber has many compact, periodic bands on the surface, perpendicular to the fiber axis. With a little drawing, the transit zone of the fiber, which is translucent, still shows some bands perpendicular to the fiber axis, but rather sparsely (Figure 2b). Finally, for the fully drawn zone of the fiber which is transparent, there are no bands simply a smooth surface (Figure 2c).

It should be noted that the banded morphology has been reported in drawing films of PEN[20] or PET/PEN copolymer[18] at temperatures close to T_g. Moreover, as we observed the white color of the LIB fibers, Kimura et al.[20] reported that the PEN film looked "turbid" with the banded morphology. In both cases,[18,20] the PEN and PET/PEN copolymer films remained amorphous or just began to crystallize when the banded structure appeared. Therefore, Abou-Kandil and Windle[18] concluded that the banding resulted from the ordering process, leading to the crystallization afterward. It was quite dramatic that we had happened to observe the banded morphology with high speed spun PET fibers 22 years before,[25] yet the observation did not draw much attention. The SEM image (see Supporting Information) indicates that the banding is just before necking through which crystallization occurs. All these results suggest that the banded structure represents a featured precursor for the crystallization of polyesters, which has been directly produced by using LIB in the melt-spinning process in this work.

Unlike the typical lamellar structure of crystallized PET or PEN, the banded structure of the white fiber spun with LIB is much larger, as shown in Figure 3a. Actually, the thickness of each band is ca. 260−300 nm for the PEN fiber. Figure 3b shows the fractured surface of the white fiber. It is clear that the periodic bands exist not only on the surface of the fiber but also inside. In contrast, the drawn, transparent fiber shows a smooth surface, with stretched fibrils inside (Figure 3c,d). The fibrils of the drawn fiber, having diameters of ca. 200−250 nm, are believed to be transformed from the banded precursor structure during hot drawing.

To obtain a full view of the inner morphology of the fibers, a focus ion beam (FIB) technology was used to cut the fibers of 20−30 μm in diameter in both radial and longitudinal directions. The high-resolution SEM images are shown in Figure 4. Surprisingly, there are many microvoids aligned in the fiber direction. The microvoids in the undrawn fiber are ellipsoid in shape, ca. 150−400 nm in long axis, and ca. 50 nm in short axis. After drawing, the microvoids are highly stretched in the drawing direction; thus, the fiber looks more

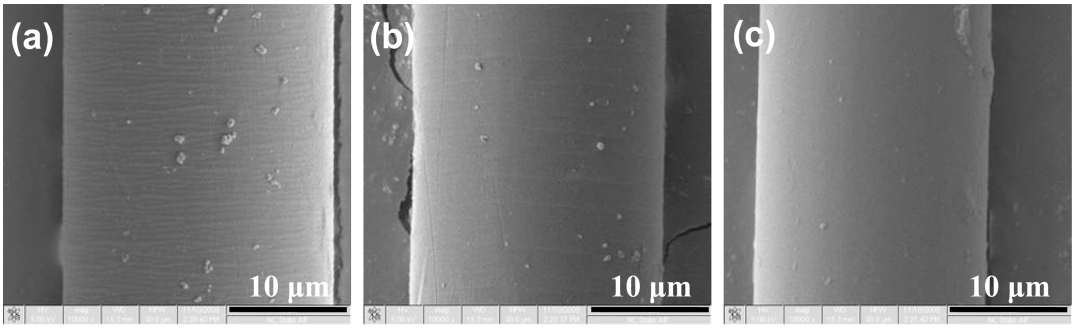

Figure 2. SEM images of PEN fibers spun with LIB (a) undrawn zone, (b) transit zone between undrawn and drawn, and (c) drawn zone.

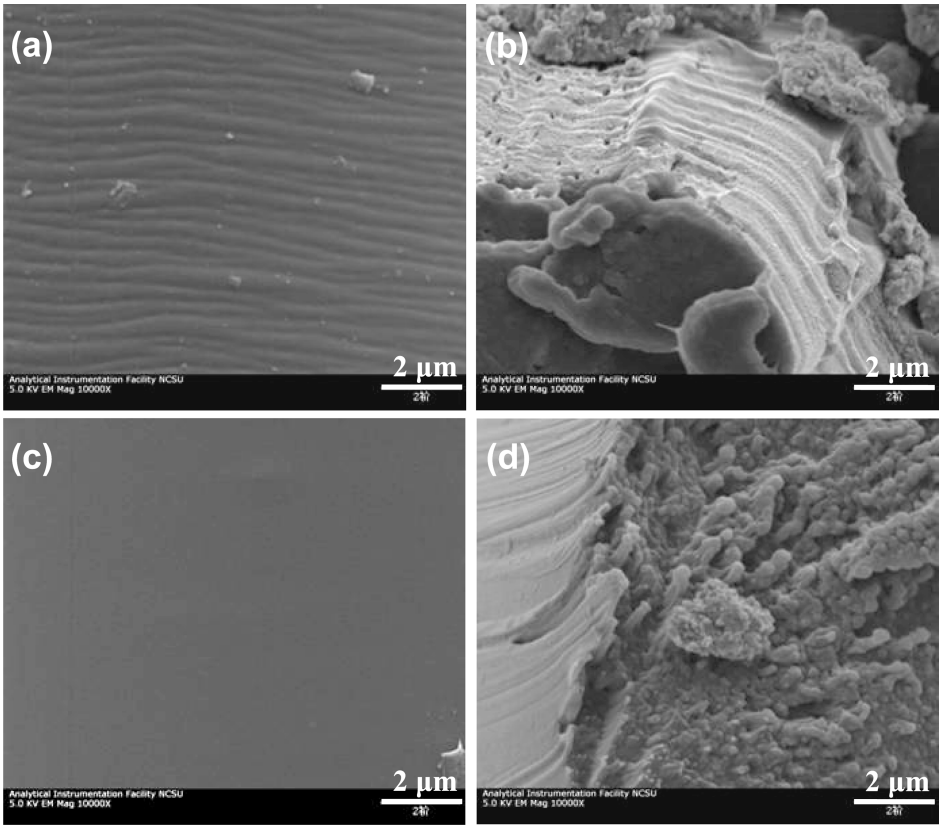

Figure 3. SEM images of PEN fibers spun with LIB (a) surface and (b) cross section of undrawn fibers; (c) surface and (d) cross section of drawn fibers.

compact, as shown in Figure 4d. The observation of microvoids well explains the low density of the undrawn LIB fiber. Moreover, the microvoids may lead to fiber whitening during spinning. Since the banded structure seems to be masked by the FIB treatment, it is obscure whether the formation of the microvoids is related with the banded structure.

At first glance one may identify the microvoids as crazing of glassy polymers experiencing plastic deformation which also leads to whitening.[26] However, as Figure 4 shows, all the microvoids are empty and aligned in the fiber direction, making them different from crazes which not only contain fibrils but also have a shape of planar cracks perpendicular to local strain direction, here the fiber direction. Recently Pawlak and Galeski[27] reviewed the cavitation process, including crazing, during tensile drawing various polymers. They further concluded that cavitation corresponded to formation of microvoids in the amorphous layers confined between crystalline lamellae.[27,28] Of most interest was, as they reported, transformation of the shape of cavities from elongated perpendicular to the drawing direction to elongated along the drawing direction as strains increased beyond a critical value (ca. 0.8−1.0).[27] Very likely the same reorientation process had occurred with the microvoids in the LIB fibers studied in this work since the fibers experienced considerably high strains while passing through LIB. In fact, the microvoids observed in this work shared the same characteristics as the cavities formed at high strains as reported by Pawlak and Galeski,[27] such as aligned along the strain direction, containing no fibrils, and having dimensions at the same level. Therefore, the microvoids in the LIB fibers should result from cavitation at high strains, instead of crazing.

According to Pawlak and Galeski,[28] the driving force for cavitation was the negative pressure generated by the stress concentration between crystalline lamellae. However, there was a lack of crystalline lamellae in the undrawn LIB fibers which contained profuse microvoids. This disclosed an important fact that the necessary condition for cavitation might not be the existence of crystalline lamellae, but formation of

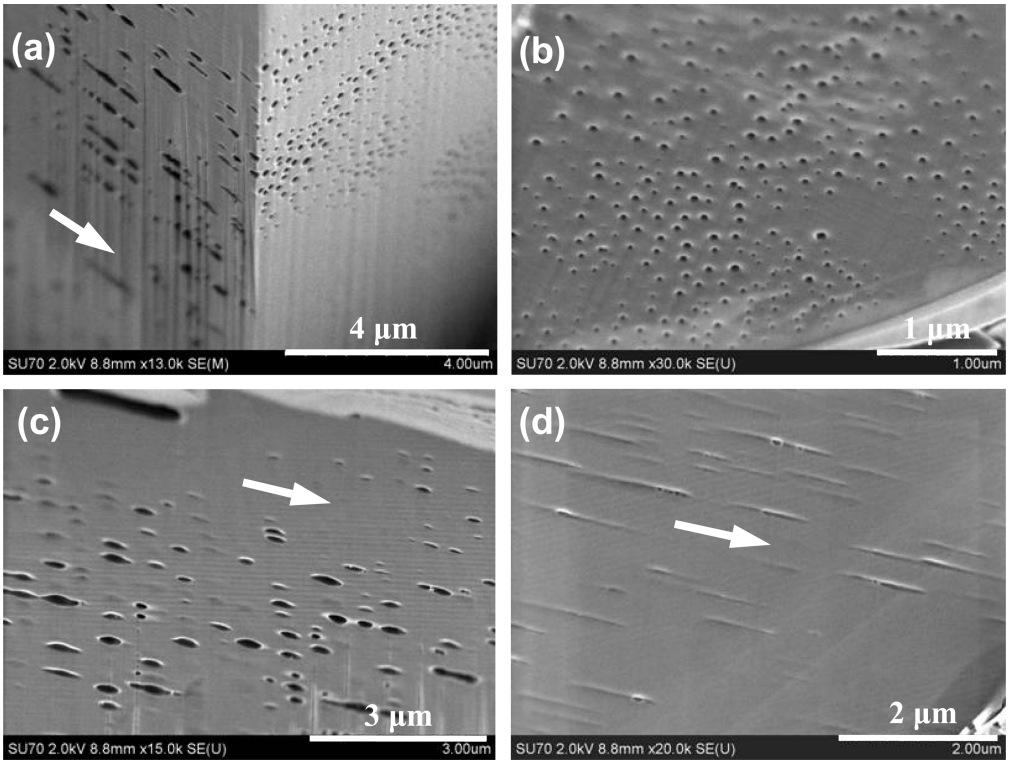

Figure 4. SEM images of FIB-treated samples (a) 2D view, (b) radial, and (c) longitudinal section of PEN undrawn fibers spun with LIB and (d) longitudinal section of drawn fibers. The arrows denote fiber direction.

any ordered structures between which the negative pressure was generated. It was worth noting that relatively low strain rates (8.3×10^{-4}–1.7×10^{-2} s^{-1}) were used in Pawlak and Galeski's work,[27,28] which permitted crystallization to occur substantially even before the activation of cavitation. Thus, it was natural to ascribe the activation of cavitation to the preexisting crystalline lamellae. In contrast, much higher strain rates were involved in high-speed spinning process, and in our case by using LIB the crystallization of PEN had not yet begun or proceeded to the detectable level of WAXD while the cavitation had predominantly occurred. This observation, associated with the significantly high tenacity as well as the banded morphology, led us to believe that the fibers spun with LIB contained highly ordered structure which was readily transformed into fibrillar crystals through a little hot drawing and was thus qualified as a precursor to crystallization.

Lying between stable amorphous and crystal phases, the precursor to crystallization, also referred to as mesophase, is featured by a highly transient formation process. It was pointed out that the major difficulty of obtaining such precursor was the exponentially increased crystallization rate with increasing temperature.[29] By using a special laboratory device to reach sufficiently high stain rate (1.7 s^{-1}) at temperatures higher than T_g, Hristov et al.[29] produced a unique morphology of PET fibers with shear bands, necks, and crazes but without crystallization, very similar to the precursor morphology observed in the present work. Taking into account that the strain rate involved in the high-speed spinning with LIB is much higher (at the level of 10^2 s^{-1}), we conjecture that the formation of the precursor structure in the LIB fibers is a reasonable extension of Hristov et al.'s observation[29] at high strain rates.

Apparently, further studies, such as in situ measurements, especially X-ray analysis, are necessary to fully understand the formation of the unique precursor morphology. However, the simultaneous occurrence of the banded structure and the microvoids has already disclosed some clues. In this study by performing melt-spinning process with LIB, white fibers with banded structure and microvoids were produced only under specific conditions, such as a high enough take-up speed (4000 m/min), a high enough liquid depth (25 cm), and a liquid temperature close to T_g of the polymers. In another case,[25] the banded structure was observed in the threadline at ultrahigh take-up speeds (> 6000 m/min). Moreover, microvoids or other defects were often formed in the fibers spun at ultrahigh speeds, as a result of high cooling rate[30] or high strain rate induced local micronecking.[29] These results suggested that the banded structure and the microvoids occurred always at high threadline tension, short deformation time, and relatively low temperature (for the melt). It was reasonable that these conditions, when well controlled, could yield a twofold effect. On the one hand, the chain ordering process was greatly improved by the high threadline tension, leading to a certain high degree of molecular orientation; on the other hand, the chain mobility was fairly limited by the low threadline temperature. As a result, the chain ordering was proceeded only locally and imperfectly within the short time, with local defects, such as the microvoids, formed and the crystallization effectively inhibited. Since the bottleneck problem of the traditional melt-spinning process, i.e., the occurrence of crystallization which interrupts the development of molecular orientation, appears to be avoided by the formation of the unique precursor morphology, we believe that this study is promising to open up a new route for producing fibers with improved properties. Future work is in planning to explore the detailed formation process of the unique precursor morphology and to extend the research to other flexible-chain, semicrystalline polymers.

Conclusions. In this work, PET and PEN fibers with unique precursor morphology were directly produced in the melt-spinning process via a liquid isothermal bath

(LIB). The fibers, which were white in color, were amorphous but oriented, as measured by WAXD. SEM observations revealed a banded structure and microvoids in the white fibers. After hot drawing, the white color of the fibers faded, accompanied by the transformation of the banded structure into a highly crystallized fibrillar structure. As a result, fibers with improved properties were produced by applying a low draw ratio.

Acknowledgment. We acknowledge the provision of research funding and polymer materials by Performance Fibers. We also appreciate Mr. F. Lundberg's assistance in sample preparation.

Supporting Information Available: Table S1 showing properties of PET fibers spun at 4000 m/min, Figure S1 showing SEM images of PET fibers spun with LIB, and Figure S2 showing SEM image of PET fiber spun at 6500 m/min. This material is available free of charge via the Internet at http://pubs.acs.org.

References and Notes

(1) Welsh, G. E.; Blundell, D. J.; Windle, A. H. *Macromolecules* **1998**, *31*, 7562.
(2) Welsh, G. E.; Blundell, D. J.; Windle, A. H. *J. Mater. Sci.* **2000**, *35*, 5225.
(3) Mahendrasingam, A.; Blundell, D. J.; Martin, C.; Fuller, W.; MacKerron, D. H.; Harvie, J. L.; Oldman, R. J.; Riekel, C. *Polymer* **2000**, *41*, 7803.
(4) Mahendrasingam, A.; Martin, C.; Fuller, W.; Blundell, D. J.; Oldman, R. J.; MacKerron, D. H.; Harvie, J. L.; Riekel, C. *Polymer* **2000**, *41*, 1217.
(5) Gorlier, E.; Haudin, J. M.; Billon, N. *Polymer* **2001**, *42*, 9541.
(6) Kawakami, D.; Ran, S. F.; Burger, C.; Fu, B.; Sics, I.; Chu, B.; Hsiao, B. S. *Macromolecules* **2003**, *36*, 9275.
(7) Kawakami, D.; Hsiao, B. S.; Ran, S. F.; Burger, C.; Fu, B.; Sics, I.; Chu, B.; Kikutani, T. *Polymer* **2004**, *45*, 905.
(8) Kawakami, D.; Hsiao, B. S.; Burger, C.; Ran, S. F.; Avila-Orta, C.; Sics, I.; Kikutani, T.; Jacob, K. I.; Chu, B. *Macromolecules* **2005**, *38*, 91.
(9) Keum, J. K.; Kim, J.; Lee, S. M.; Song, H. H.; Son, Y. K.; Choi, J. I.; Im, S. S. *Macromolecules* **2003**, *36*, 9873.
(10) Mahendrasingam, A.; Blundell, D. J.; Wright, A. K.; Urban, V.; Narayanan, T.; Fuller, W. *Polymer* **2003**, *44*, 5915.
(11) Asano, T.; Calleja, F. J. B.; Flores, A.; Tanigaki, M.; Mina, M. F.; Sawatari, C.; Itagaki, H.; Takahashi, H.; Hatta, I. *Polymer* **1999**, *40*, 6475.
(12) Abou-Kandil, A. I.; Windle, A. H. *Polymer* **2007**, *48*, 5069.
(13) Kawakami, D.; Ran, S. F.; Burger, C.; Avila-Orta, C.; Sics, I.; Chu, B.; Hsiao, B. S.; Kikutani, T. *Macromolecules* **2006**, *39*, 2909.
(14) Gutierrez, M. C. G.; Karger-Kocsis, J.; Riekel, C. *Macromolecules* **2002**, *35*, 7320.
(15) Jakeways, R.; Klein, J. L.; Ward, I. M. *Polymer* **1996**, *37*, 3761.
(16) Saw, C. K.; Menczel, J.; Choe, E. W.; Hughes, O. R. *SPE Annu. Tech. Conf.* **1997**, *2*, 1610.
(17) Blundell, D. J.; Mahendrasingam, A.; Martin, C.; Fuller, W. *J. Mater. Sci.* **2000**, *35*, 5057.
(18) Abou-Kandil, A. I.; Windle, A. H. *Polymer* **2007**, *48*, 4824.
(19) Shioya, M.; Kawazoe, T.; Okazaki, R.; Suei, T.; Sakurai, S.; Yamamoto, K.; Kikutani, T. *Macromolecules* **2008**, *41*, 4758.
(20) Kimura, T.; Tokunaga, H.; Ito, E.; Niino, H.; Yabe, A. *Polym. J.* **1999**, *31*, 524.
(21) Wu, G.; Zhou, Q.; Chen, J. Y.; Hotter, J. F.; Tucker, P. A.; Cuculo, J. A. *J. Appl. Polym. Sci.* **1995**, *55*, 1275.
(22) Tonelli, A. E. *Polymer* **2002**, *43*, 637.
(23) Abou-Kandil, A. I.; Goldbeck-Wood, G.; Windle, A. H. *Macromolecules* **2007**, *40*, 6448.
(24) Chen, P.; Kotek, R. *Polym. Rev.* **2008**, *48*, 392.
(25) Cuculo, J. A.; Lundberg, F. Unpublished data (see Supporting Information).
(26) Kausch, H. H.; Halary, J. L. In *Mechanical Properties of Polymers Based on Nanostructure and Morphology*; Michler, G. H., Balta-Calleja, F. J., Eds.; Taylor & Francis: Boca Raton, FL, 2005; Chapter 4.
(27) Pawlak, A.; Galeski, A. *Macromolecules* **2008**, *41*, 2839.
(28) Pawlak, A.; Galeski, A. *Macromolecules* **2005**, *38*, 9688.
(29) Hristov, H. A.; Hearle, J. W. S.; Schultz, J. M.; Kennedy, A. D. *J. Polym. Sci., Part B: Polym. Phys.* **1995**, *33*, 125.
(30) Wu, G.; Li, Q. C.; Cuculo, J. A. *Polymer* **2000**, *41*, 8139.